

Multivariable Robust Control for Two-Zone Thermal Plate System

Poom Jatunitanon*, Withit Chatlatanagulchai

¹Control of Robot and Vibration Laboratory (CRVLAB), Department of Mechanical Engineering, Faculty of Engineering, Kasetsart University, 50 Ngam Wong Wan Rd, Lat Yao, Chatuchak, Bangkok, 10900

*Corresponding Author: poom_legend@hotmail.com, Telephone Number 086-376-4025, Fax. Number 02-579-4576

Abstract

There are two major classifications for the controllers of multivariable plants: the decentralized controller (diagonal controller) and the full-matrix controller. The decentralized controller is a diagonal transfer function matrix; therefore, it is more suitable for a diagonal plant because then the plant to be controlled is essentially a collection of independent sub-plants. If the off-diagonal elements in the plant are large, the performance of the decentralized controller may be poor because no attempt is made to counteract the interactions. This paper compares the decentralized controller with the full-matrix controller of a two-zone thermal plate system. The system has two inputs and two outputs. The inputs are voltages applied to each power drive circuit to generate heat energy for thermoelectric zone. The outputs are temperature of two-zone thermoelectric module. The two thermal plate zones are placed next to each other causing interactions between inputs and outputs. This paper proposes a centralized H_∞ control strategy and compares it with conventional decentralized control, using a PI controller for each thermal zone. Simulation and experimental results show that the proposed method handles the interaction between two thermal zones better than the decentralized control, resulting in significantly more accurate tracking of the temperature.

Keywords: H_∞ Control, Decentralized Control, Thermoelectric Module, Thermal Plate.

1. Introduction

A diagonal control works well if the selection of pairings between inputs and outputs are appropriate. In plant transfer function matrix, the off-diagonal elements represent the relationship between inputs and outputs for sub-plants are the cause of interaction. When the off-diagonal elements are large, they may cause instability and full multivariable control is required for dealing with an interaction effect.

For studying the interaction effect in the multivariable plants, this work use two-zone

thermal plate as the demo plant and set condition of interaction by placed thermal plate next to another plate.

In addition, there is no complete knowledge of zone's thermal system because system parameters vary when system operates in different working condition. Therefore, the controller should handle all uncertain parameters.

Several techniques have been proposed in the literature for temperature control of the multi-zone temperature plate. In [1], Ho, W.K., Tay, A., Cheng, M. and Kiew, C.M. proposed optimal PI

feed forward to optimize a control signal and improve transient response by using optimal gain in each thermal zone in multiple zone thermal system. In [2], Tay, A., Tan, K.K., Zhao, S. and Lee, T.H. proposed simulation study of predictive ratio control of multi-zone thermal for improve traditional ratio control because the ratio control approach does not deal with an interaction between temperature zones.

Controllers based on model predictive techniques, such as model predictive control (MPC), multiplexed MPC (MMPC) and fast MPC were also developed to serve the requirements of the system [3]. In general, MPC solves a finite-time constrained optimization online to obtain the control input to minimize future tracking error. MMPC was developed for online reduction of computational load of MPC by using faster sampling for better performance. The effects of disturbances were decreased significantly by using feed-forward.

In addition to procedures discussed above, since the multi-zone thermal system is complicated, efficient control strategies should be used such as H_{∞} control and linear quadratic regulator (LQR) because the centralized multi-input-multi-output (MIMO) control can compensate for the interaction caused by the temperature gradient between each zone. In [4], H. Hamane, K. Matuki, F. Hiroki and K. Miyazaki proposed a robust controller for MIMO thermal twin screw extruder system for the interaction between temperature zones. The proposed method is successful in solving the interaction problem for MIMO temperature process [4]. From the literature, many researchers developed control algorithms to deal with plant uncertainty of the

system and reject a disturbance. As a result, MIMO robust controller should be implemented because this algorithm has the ability to deal with model uncertainty, to reject a disturbance and to compensate for the interaction caused by energy transfer between each zone.

The proposed H_{∞} control strategy is verified in both simulation and experiment tests. A comparison study between H_{∞} control and decentralized SISO PI control, based on control performance and robustness, is presented.

2. Hardware Setup

The implementation of hardware and software in developing the control algorithm for two thermal zones can be seen from Fig. 1 The testing apparatus contains two thermoelectric modules for two temperature zones.

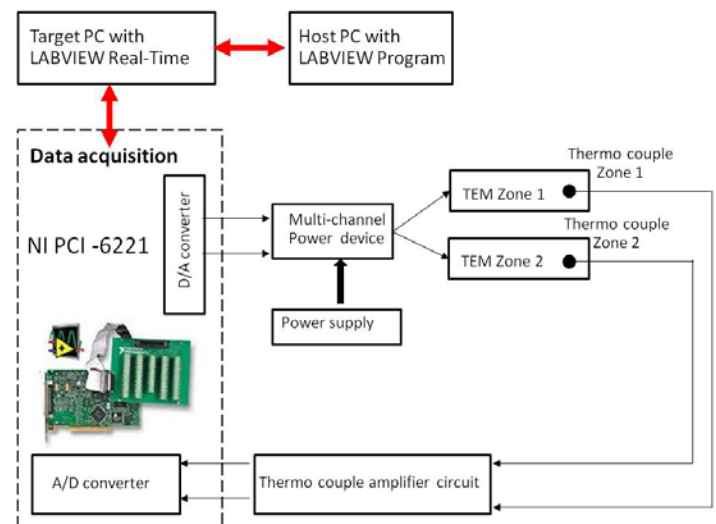


Fig. 1 Implementation of hardware and software

Each zone has thermocouple sensor for measuring dynamic of temperature. This experiment use NI PCI-6221 as data acquisition for converting the analog signal from amplified temperature signal to a digital signal for

calculating in a target computer with Lab View Real-Time software. The host computer is used to develop control algorithm such as, H_∞ control and SISO PI controller.

After control signal activates the power device, the power supply sends the voltage source, depending on a control signal to each thermoelectric zone. This experiment uses the multi-channel power device for supplying two-zone of thermoelectric module. The picture of test apparatus can be seen from Fig. 2.

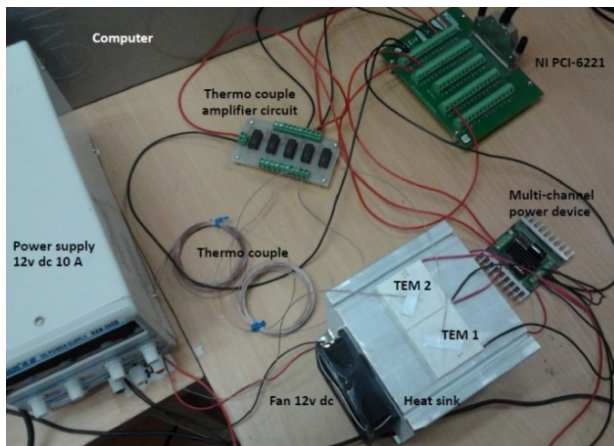


Fig. 2 The test apparatus.

3. System Modeling

The steady-state model of two-zone thermal plate system can be determined by energy balance between thermal zones as shown in Fig. 3. Each zone transfers energy to another zone and transfers to ambient temperature so this system can be written as a steady-state model of thermal system due to energy balance as shown in Eqs. (1) – (2) for zone 1, 2, respectively.

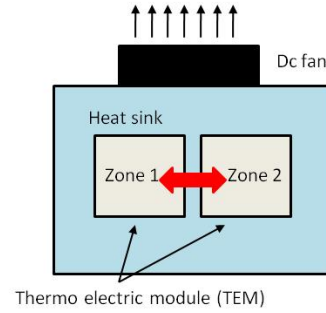


Fig. 3 Energy transfer between thermo electric zones.

$$C_1 \dot{\theta}_1(t) = u_1(t) - \frac{1}{R_1} \theta_1(t) + \frac{1}{r_{12}} \theta_2(t) \quad (1)$$

$$C_2 \dot{\theta}_2(t) = u_2(t) + \frac{1}{r_{21}} \theta_1(t) - \frac{1}{R_2} \theta_2(t) \quad (2)$$

where

θ_i is temperature of zone i

R_i is thermal resistance of zone i

r_{ij} is thermal resistance between zone i and j

u_i is control effort of zone i .

Subscripts i and j are numbers of zone in the system.

From mathematical models (1) and (2), the interaction between thermal zones is caused by temperature difference, for example, when $\theta_1(t) \neq \theta_2(t)$. Energy transfers from high-temperature source to low-temperature source, so the output temperatures of each zone can be oscillated from reference temperature signal by interaction effect.

3.1 System Identification Process

The essential parameters of multi input multi output two-zone thermal system can be extracted by open-loop step test [10] as shown in Fig. 4. System inputs and outputs are recorded as real time for determining system parameters.



Fig. 4 Open-loop step test of MIMO plant

This work use transfer function matrix for finding steady-state gain (K_{ij}) and time constant parameter (τ_{ij}) of the first order transfer function in transfer function matrix as shown in Eq. (3):

$$\begin{bmatrix} Y_1 \\ Y_2 \end{bmatrix} = \begin{bmatrix} \frac{K_{11}}{\tau_{11}S+1} & \frac{K_{12}}{\tau_{12}S+1} \\ \frac{K_{21}}{\tau_{21}S+1} & \frac{K_{22}}{\tau_{22}S+1} \end{bmatrix} \begin{bmatrix} U_1 \\ U_2 \end{bmatrix}. \quad (3)$$

The uncertain parameter of steady-state gain (K_{ij}) in transfer function matrix can be seen in Table. 1.

Table. 1 Uncertainty of steady-state gain (K_{ij})

G_{ij}	Steady-state gain (K_{ij})		
	Min. value	Nom. value	Max. value
G_{11}	12.60	18.47	26.40
G_{12}	10.17	20.59	39.70
G_{21}	9.56	20.75	36.64
G_{22}	9.73	17.12	21.45

The uncertain parameter of time constant (τ_{ij}) in transfer function matrix can be seen in Table. 2.

Table. 2 Uncertainty of time constant (τ_{ij})

G_{ij}	Time constant (τ_{ij})		
	Min. value	Nom. value	Max. value
G_{11}	16.30	30.205	44.37
G_{12}	21.40	47.725	76.40
G_{21}	11.84	39.328	79.80
G_{22}	16.33	17.840	19.48

Therefore, nominal transfer function matrix is shown in Eq. (4):

$$\begin{bmatrix} Y_1 \\ Y_2 \end{bmatrix} = \begin{bmatrix} \frac{18.47}{30.205S+1} & \frac{20.59}{47.725S+1} \\ \frac{20.75}{39.328S+1} & \frac{17.12}{17.84S+1} \end{bmatrix} \begin{bmatrix} U_1 \\ U_2 \end{bmatrix}. \quad (4)$$

4. Controller Synthesis

A centralized multivariable robust controller is proposed in this work. The controller algorithm is H_∞ control based on multiplicative output uncertainty using mix-sensitivity approach to deal with system uncertainty.

Fig. 5 shows the general formulation of H_∞ control, where $P(s)$ is generalized plant, $K(s)$ is controller, u represents the control signal, v is measured variable, w is called the exogenous signal such as a reference signal and z stands for error variable.

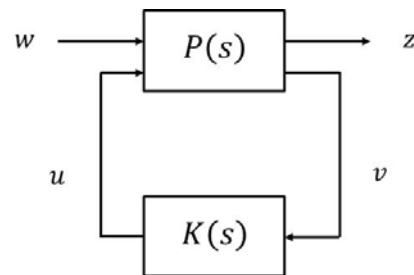


Fig. 5 General formulation of H_∞ control.

Some solutions, formulating as optimization problems, have been proposed, for example, Doyle *et al.* [6], Zhou and Doyle [7], Feng [8], Skogestad [11] and Chatlatanagulchai [12]. The synthesis method has been implemented in well-known software such as Matlab.

The $S/KS/T$ mixed sensitivity problem uses generalized plant $P(S)$ as shown in Fig. 6. The expression of the resulting closed-loop transfer function, $T_{zw}(S)$, is as follows:

$$T_{zw}(S) = \begin{bmatrix} W_S(s)S_o(s) \\ W_{KS}(s)K(s)S_o(s) \\ W_T(s)T_o(s) \end{bmatrix}. \quad (5)$$

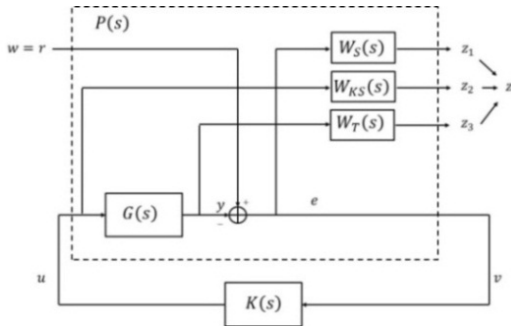


Fig. 6 $S/KS/T$ mixed sensitivity.

Where $S_o(s)$ is the output sensitivity transfer function matrix, $T_o(s)$ is the output complementary sensitivity transfer function matrix, and $K(s)S_o(s)$ is the control sensitivity transfer matrix. The equation of each sensitivity transfer function matrix can be seen in Eqs. (6) – (8), respectively:

$$S_o(s) = (I + G(s)K(s))^{-1} \quad (6)$$

$$T_o(s) = G(s)K(s)(I + G(s)K(s))^{-1} \quad (7)$$

$$K(s)S_o(s) = K(s)(I + G(s)K(s))^{-1}. \quad (8)$$

The factors $W_T(s)$ and $W_S(s)$ are desired shapes for $T_o(s)$ and $S_o(s)$, which are complementary sensitivity function for tracking problem and sensitivity function for improving the performance of the system, respectively.

In addition, $W_{KS}(s)$ is used for avoiding some numerical problems in the synthesis process.

The magnitude of $W_T(s)$ weighting matrix should be as upper bound of maximum singular values of the multiplicative output uncertainty. The

multiplicative output uncertainty can be estimated as

$$\hat{E}o_{Pi}(s) = (\hat{G}_{Pi}(s) - \hat{G}(s))\hat{G}(s)^{-1}, \quad (9)$$

where $\hat{G}(s)$ is nominal model and $\hat{G}_{Pi}(s)$ is each of non-nominal model from working condition Pi . Fig. 7 shows the maximum singular values of each non-nominal working condition.

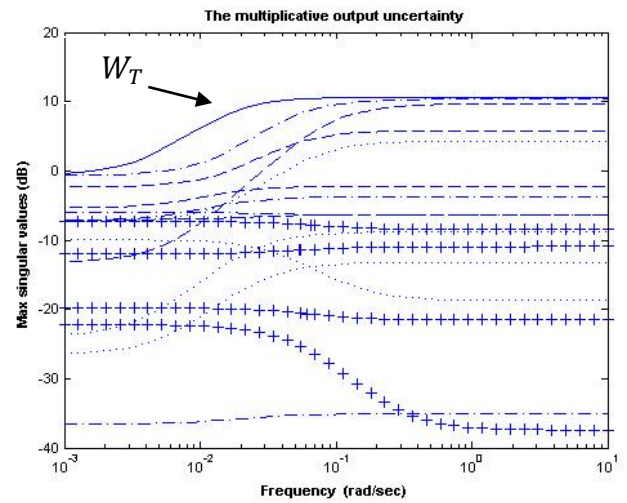


Fig. 7 $W_T(s)$ matrix (solid line) as an upper bound of each maximum singular values of multiplicative output uncertainty.

Matrix $W_T(s)$ is designed as a square diagonal matrix as

$$W_T(s) = \begin{bmatrix} \frac{3.4s+0.014}{s+0.015} & 0 \\ 0 & \frac{3.4s+0.014}{s+0.015} \end{bmatrix}. \quad (10)$$

The magnitude of this transfer function is plotted in Fig. 7.

Matrix $W_S(s)$ is designed as a square diagonal matrix of transfer function as

$$W_S(s) = \begin{bmatrix} \frac{\alpha_i s + 10^{(\kappa_i - 1)} \omega_T}{s + \beta_i 10^{(\kappa_i - 1)} \omega_T} & 0 \\ 0 & \frac{\alpha_i s + 10^{(\kappa_i - 1)} \omega_T}{s + \beta_i 10^{(\kappa_i - 1)} \omega_T} \end{bmatrix}, \quad (11)$$

according to design rules in [5].

ω_T is crossover frequency from Fig. 7. The crossover frequency equals to 0.383 rad/sec. Parameters α_i and β_i represent the transfer function gain at high and low frequency when $i = T_{Z1}, T_{Z2}$, respectively.

To avoid numerical problem in the synthesis algorithm, this work sets weight $W_{KS}(s)$ to identity matrix, as

$$W_{KS}(s) = \begin{bmatrix} 1 & 0 \\ 0 & 1 \end{bmatrix}. \quad (12)$$

5. Simulation Study

H_∞ and SISO PI controller are implemented in Matlab for studying the tracking performance of output temperature.

Fig. 8 shows the simulation results of thermal zone 1 and Fig. 9 shows simulation results of thermal zone 2.

From Fig. 8, all of the controller can track reference signal in three operating conditions at thermal zone 1. SISO PI controller is the best in rising time when reference signal is changed, but this control algorithm has some overshoot and steady-state error.

However, Fig. 9 shows the temperature response of thermal zone 2 when SISO PI is used as the controller. The output temperature has a larger overshoot than MIMO centralized controller when reference signal is changed in thermal zone 1. This effect is caused by interaction between zones and MIMO centralized changes response a little when reference signal changes.

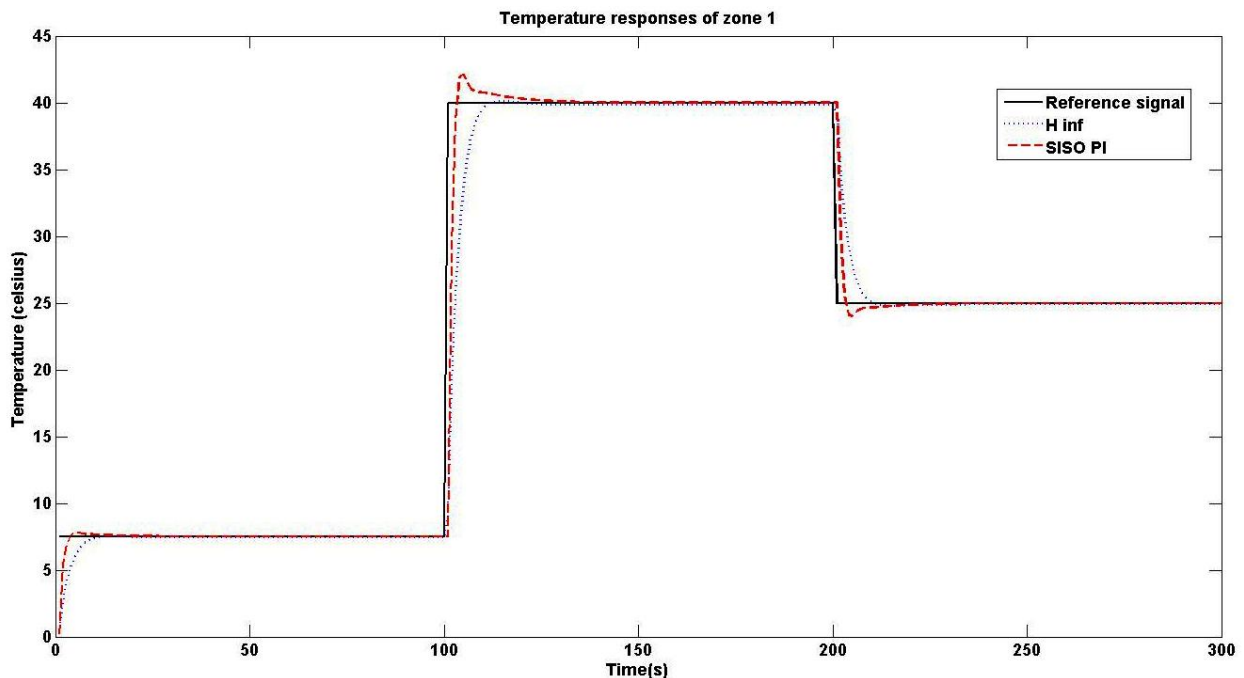


Fig. 8 Simulation comparison between using SISO PI (dash line) and H_∞ (dot line) at thermal zone 1.

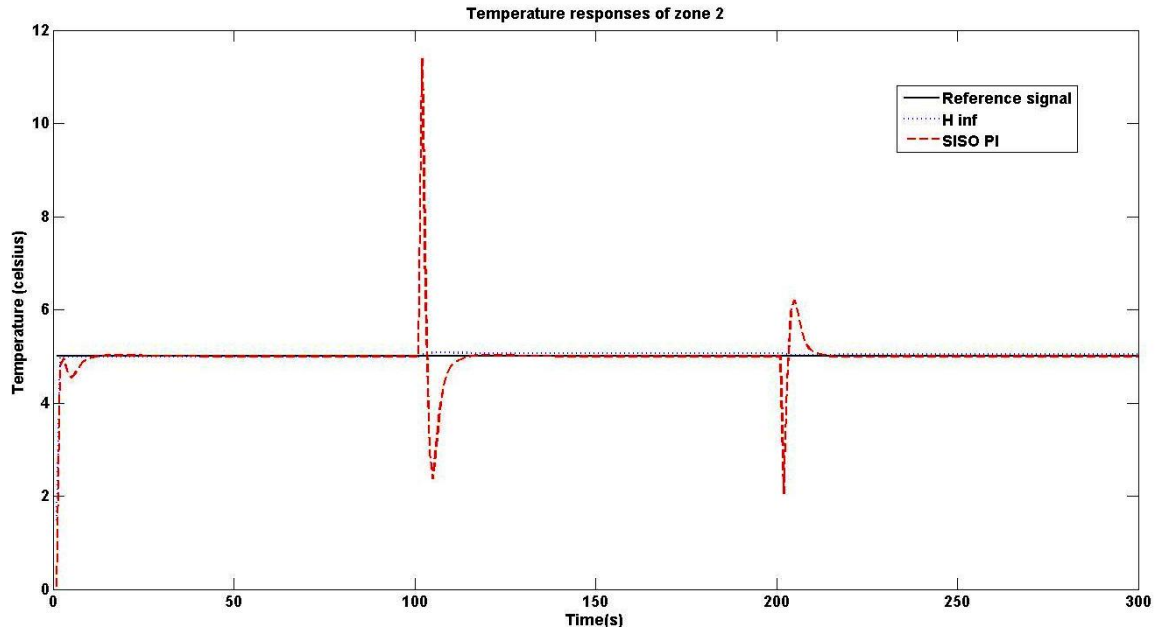


Fig. 9 Simulation comparison between using SISO PI (dash line) and H_{∞} (dot line) at thermal zone 2.

6. Experimental Study

This experiment tests interaction effect between two thermal zones. For specifying the interaction condition, this test uses three working conditions at thermal zone 1 and one working condition at zone 2 for studying performance of SISO PI and H_{∞} controller.

Fig. 10 shows the experimental study for tracking performance of two controllers. It is clear from this experiment results that the proposed H_{∞} controller is better than SISO PI controller in terms of rejecting disturbance from surrounding areas' temperature and having small steady-state error. However, the rising times of two controllers are the same. In the final period, temperature decreases sharply and then is kept at final reference value as shown in Fig. 10.

The line graph of Fig. 11 shows temperature response of thermal zone 2 when using SISO PI and H_{∞} controller of one reference signal at 10 °C. Overall, it is clear that H_{∞} controller can keep temperature output of zone 2 at reference signal better than SISO PI controller. In addition, the temperature when using SISO PI controller fluctuates significantly between 10 – 12 °C from 100 seconds to 200 seconds due to the temperature of thermal zone 1 is changed to 40 °C, so the high energy in zone 1 is transferred to low temperature source at zone 2 and SISO PI controller cannot deal with interaction effect like that of H_{∞} control. The full matrix controller for implementation is

$$K(s) = \begin{bmatrix} K_{11} & K_{12} \\ K_{21} & K_{22} \end{bmatrix} \quad (13)$$

Where

$$K_{11} = \frac{-0.08095s^6 - 2.719s^5 - 0.3515s^4 - 0.01742s^3 - 0.000413s^2 - 4.7s - 2.058}{s^7 + 55.82s^6 + 63.96s^5 + 25.58s^4 + 4.029s^3 + 0.2015s^2 + 0.00366s + 0.00219}$$

$$K_{12} = \frac{34.25s^7 + 40.42s^6 + 24.68s^5 + 6.763s^4 + 0.55s^3 + 0.0184s^2 + 0.00026s + 1.36}{s^8 + 439s^7 + 2.14s^6 + 25.58s^4 + 2.4s^5 + 9800s^4 + 1543s^3 + 77s^2 + 1.4s + 0.083}$$

$$K_{21} = \frac{0.01s^6 + 2.4s^5 + 0.35s^4 + 0.018s^3 + 0.00044s^2 + 0.000584s + 0.000002233}{s^7 + 55.82s^6 + 63.96s^5 + 25.58s^4 + 4.029s^3 + 0.2015s^2 + 0.00366s + 0.00219}$$

$$K_{22} = \frac{37.06s^7 + 45.95s^6 + 13.3s^5 + 0.344s^4 - 0.0414s^3 - 0.00195s^2 + 0.00028s - 1.323}{s^8 + 439s^7 + 2.14s^6 + 25.58s^4 + 2.4s^5 + 9800s^4 + 1543s^3 + 77s^2 + 1.4s + 0.083}$$

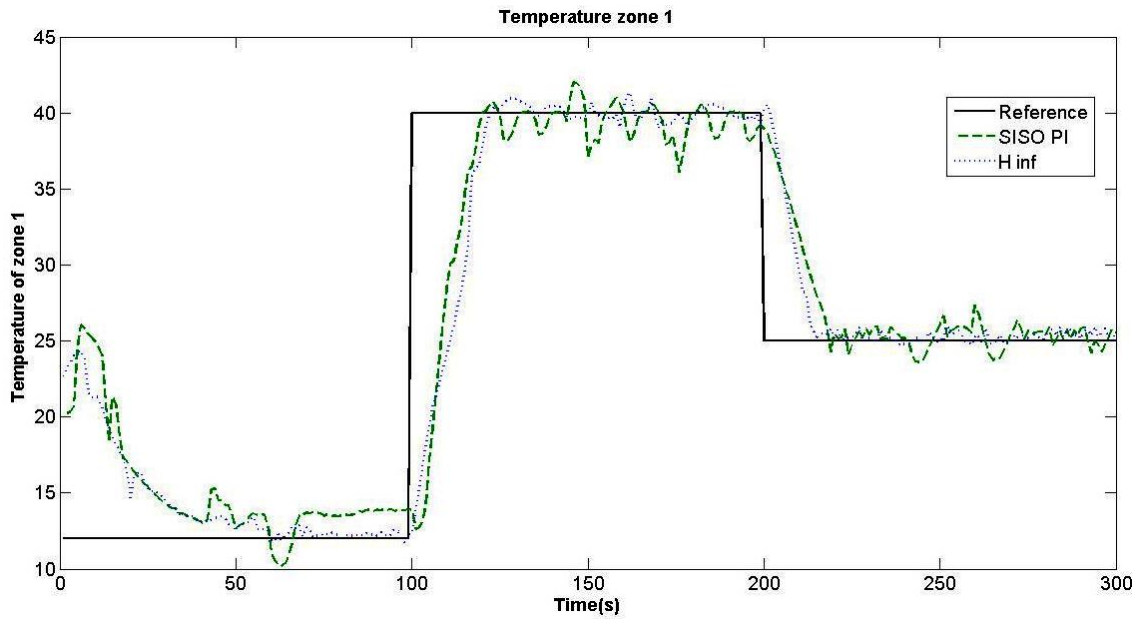


Fig. 10 Tracking performance of different controllers: H_{∞} (dot line) and SISO PI (dash line).

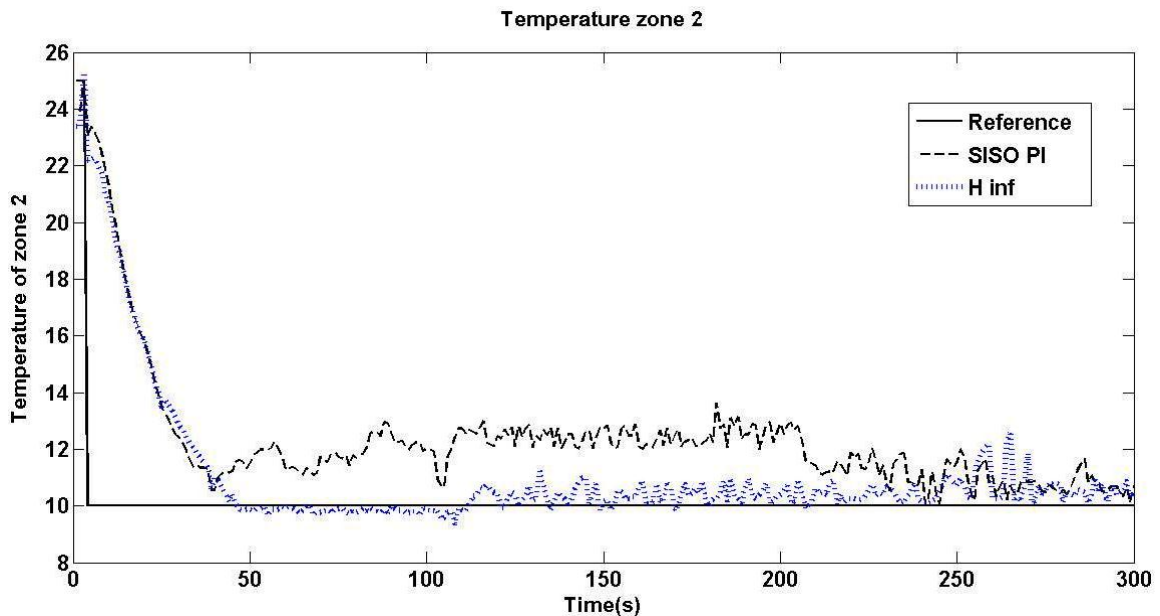


Fig. 11 Temperature response of thermal zone 2: H_{∞} (dot line) and SISO PI (dash line).

The decentralized PI controller is designed base on robustness with uncertain parameters according to Katshuhiko [9]. The complementary sensitivity function of PI controller (T_{PI}) can be written as

$$T_{PI} = \frac{K_{PI}G_{ij}}{1+K_{PI}G_{ij}} \quad (14)$$

The system is guaranteed to be stable as long as T_{PI} satisfy inequality (15).

$$\left| \frac{\Delta G}{G_N} \right| < \left| \frac{1}{T_{PI}} \right| \quad (15)$$

Where ΔG is a difference between non-nominal model and nominal model (G_N). This means that as long as the modeling error remains below $1/T_{PI}$ as shown in Fig. 12, the system is stable [9].

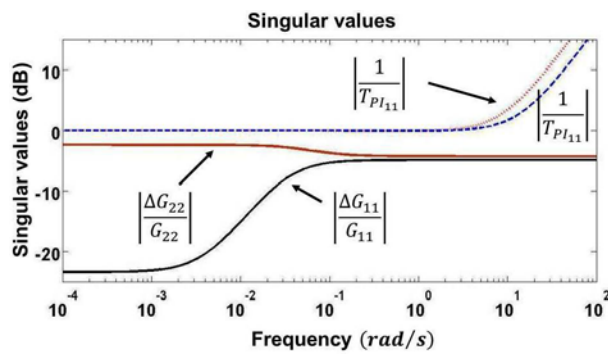


Fig. 12 $\left| \frac{1}{T_{PI11}} \right|$ and $\left| \frac{1}{T_{PI22}} \right|$ (dash-line) as an upper bound of modeling error ΔG_{11} and ΔG_{22}

The diagonal matrix of decentralized PI controller for satisfying the inequity (15) can be written as

$$\begin{bmatrix} \frac{15.7S+2.4}{S} & 0 \\ 0 & \frac{14.8S+1.9}{S} \end{bmatrix} \quad (15)$$

7. Conclusion

This apparatus is designed to study interaction effect between two thermal zones. Robust MIMO controller is developed based on the H_∞ mixed sensitivity problem for dealing with effect of uncertainty and interaction effect between two thermal zones.

Simulation and experimental results show that the performance of proposed controller, for attenuating disturbance and dealing with interaction problem between two thermal zones, is better than decentralized PI controller.

8. References

- [1] Ho, W.K., Tay, A., Cheng, M. and Kiew, C.M. (2007). Optimal feed-forward control for multizone baking in microlithography, *Industrial and Engineering Chemistry Research*, vol.46, pp. 3623 – 3628.
- [2] Tay, A., Tan, K.K., Zhao, S. and Lee, T.H. (2008). Predictive ratio control of multi-zone thermal processing system in lithography, *The International Federation of Automatic Control*, vol.46, pp. 10863 – 10868.
- [3] Ling, K.V., Ho, W.K., Wu, B.F., Andreas, Wu. and Yan, H. (2009). Multiplexed MPC for Multi-zone Thermal Processing in Semiconductor Manufacturing, *IEEE Transaction on control system technology*, vol.18, pp. 1371–1380.
- [4] Hamane, H., Matuki, K., Hiroki, F. and Miyazaki, K. (2010). Thermal MIMO controller for set point regulation and load disturbance rejection, *Control Engineering Practice*, vol.18, pp. 198 – 208.
- [5] Ortega, M.G. and Rubio, F.R. (2004). Systematic design of weighing matrices for H_∞

mixed sensitivity problem, *Journal of process control*, vol.14, pp. 89 – 98.

[6] Doyle, J.C. Glover, K., Khargonekar, P.P. and Francis, B.A. (1989). State-space solutions to standard H-2 and H-infinity control problem, *IEEE Transaction on Automatic Control*, vol.34, pp. 831 – 847.

[7] Zhou, K. and Doyle, J.C. (1998). *Essentials of robust control*, Prentice-Hall, New York.

[8] Feng, L. (2007). *Robust control design an optimal approach*, Wiley& sons, England.

[9] Katsuhiko, O. (1997). *Modern Control Engineering*, Prentice-Hall, New jersey.

[10] Lennart, L. (1999). *System Identification Theory for the User*, Prentice-Hall, New jersey.

[11] Skogestad, S. and Postlethwaite, I. (2001). *Multivariable Feedback Control Analysis and Design*, Wiley& sons, England.

[12] Chatlatanagulchai, W. (2011). *System modeling and control*, Kasetsart university, Thailand.